

## Performance of Various Length-to-Diameter Ratio of Thermal Energy Storage Tank: A Convergence Test

M.S.A. Fouzi<sup>1</sup>, N.A.M. Amin<sup>1\*</sup>, A. Mohamad<sup>1</sup>, M.S. Mohamad<sup>1</sup>, M.H. Basha<sup>1</sup>,  
A.A. Rahman<sup>1</sup>, M.S. Bakar<sup>1</sup>, M.A. Karim<sup>1</sup>, I. Zaman<sup>2</sup>

<sup>1</sup> Mechanical Engineering Programme, Faculty of Mechanical Engineering & Technology,  
Universiti Malaysia Perlis (UniMAP), Pauh Putra Main Campus, Perlis, Arau, 02600, MALAYSIA

<sup>2</sup> Faculty of Mechanical and Manufacturing Engineering,  
Universiti Tun Hussein Onn Malaysia, 86400, Parit Raja, Johor, MALAYSIA

\*Corresponding Author: [nasrulamri.mohdamin@unimap.edu.my](mailto:nasrulamri.mohdamin@unimap.edu.my)

DOI: <https://doi.org/10.30880/ijie.2024.16.02.023>

### Article Info

Received: 14 December 2023

Accepted: 17 June 2024

Available online: 23 June 2024

### Keywords

Thermal energy storage, phase change material, computational fluid dynamics, convergence

### Abstract

Thermal Energy Storage (TES) is a technique that stores thermal energy, accomplished by changing the temperature of a storage medium, such as a phase change material (PCM), for later use in various applications, for example, heating and cooling or power generation. The heat energy that is saved is usually kept in the storage medium. This study investigates how the performance of the TES tank is affected by the ratio of length to diameter. The research focuses on how the ratio affects the convergence test while the PCM0 (water-ice) used in TES starts to release latent heat into the air. Five models were designed by using CATIA software and the analysis was conducted in ANSYS CFD software. Convergence tests were conducted to validate the accuracy of the obtained simulation results. Two additional criteria, namely temperature and ice mass fraction, were also analysed to evaluate the performance of the TES tanks. The investigation of the TES tank using five different models has shown that each model reaches a constant temperature of 0°C during the melting phase, but at different time intervals. Model 1 reaches this temperature the fastest, followed by Model 2, Model 3, Model 4, and finally Model 5. A model that reached the constant temperature first indicated a more efficient discharging process, as it signified a faster rate of ice melting and thermal energy release. In terms of ice mass fraction, Model 1 retained a significant amount of solid ice (0.9968), with noticeable melting. Model 5, on the other hand, showed minimal melting and better preservation of solid ice (0.9992). Considering temperature, ice mass fraction and ease of convergence, Model 1 performed the best, when the solidified PCM0 was melting faster while maintaining a substantial amount of solid ice in the TES tank. The present study was successfully developed and compared various TES configurations while satisfying the convergence criteria set in the simulation. To conclude with, the results showcase the performance differences based on pipe size. These discoveries contribute to refining tube-type TES tanks and their design for thermal energy storage systems.

## 1. Introduction

Thermal energy storage (TES) is a method of acquiring and storing heat energy for later use in cooling, heating, or power generation. TES systems ensure a more stable energy supply through its ability to store energy during low demand and releasing the energy back throughout high demand periods [1]. Different materials with different thermal properties can be used in the applications of TES, presenting versatility. These systems are usually applied in both industrial and building sectors, resulting to an efficient energy management strategy [2]. The choice of phase change material (PCM) and heat storage container geometry is vital in thermal energy storage systems. Extensive research has been made upon the investigation on effectiveness of the cylindrical, shell-and-tube design. A lot of factors impacting the performance of this model, such as the heat transfer fluid, physical dimensions, presence of natural convection, and inclusion of fins. The melting and solidifying process is known to be affected by fluid's flow rate and temperature. The dimensions of the TES system, including the ratio of shell to tube radius, thickness, size, and tube radius, all contribute to the system's effectiveness [3][4].

The focus of research on low-heat thermal energy storage (LHTES) systems is primarily on efficient shell-and-tube designs that capable of minimizing the heat loss. The cylindrical shell-and-tube configuration offers greater heat transfer rates and faster energy storage. The ratio of efficient energy storage compares actual stored heat to an ideal water storage tank. It influences the development of LHTES systems [5]. To analyze the influence of different tube configurations on performance, a computational fluid dynamics (CFD) simulation was conducted to deliver a dataset of the optimal length-to-diameter ratio in a thermal storage tank.

### 1.1 Research Background

Thermal energy storage is a popular method of storing energy for short-term use. Nevertheless, there is always the case of redundant amount of PCM used in the system and low heat transfer in unoptimized TESs. To make thermal energy storage in a good performance, many things need to be considered, such as the type of materials in use, volume of PCM, number of the coil, length-to-diameter ratio in various sizes and much more. In this case, it is unavoidable to improve the efficiency of the thermal energy storage for the TES design to be optimized, by making sure the size.

Phase change materials are recognized for their capability of storing a considerable amount of thermal energy during a phase change process typically between solid and liquid states, at a specific temperature [6]. The main benefits of systems that utilize phase change for storage are the significant capacity for heat storage and the capability to keep a steady temperature throughout both the charging and discharging cycles [7][8]. This paper studies the evolution of solid-liquid phase changes thermal energy storage and examines three key areas: materials, heat transfer, and applications.

Additionally, the thermophysical properties of materials commonly used as potential PCM are discussed [9]. There are many different types of PCMs, with the main distinction being between inorganic and organic materials. Some of the Phase Change Materials that are most typically utilised in technical applications are paraffins (organic), fatty acids (organic) and salt hydrates (inorganic).

Paraffins are a group of pure alkanes that have varying phase change temperatures. However, the small thermal conductivity of paraffins in comparison to inorganic materials restricts the number of paraffins that can be employed in practical solar energy applications [9]. To improve the thermal performance of the LHTES unit, a composite PCM is employed [10], this is achieved by incorporating copper foam into pure paraffin. A low-heat thermal energy storage systems (LHTES) capacity to function effectively is closely related to the utilised phase change material's (PCM) thermal properties. According to Banoqitah et al. [11], in the investigation on the nanocomposite stability embedded in the organic PCM (paraffin wax) alongside its properties' augmentation, a few numbers of nanoparticle types were used found to improve paraffin wax properties which included nanotubes [12], zinc oxide [13], graphene oxide [14], titanium (III) oxide [15] and titanium dioxide [16]. Due to its advantageous thermo-physical characteristics, pure paraffin is a common PCM because of its high latent heat, thermal and chemical stability, and environmentally friendly nature, making it suitable for LHTES systems that operate in the 10 to 90°C temperature range [17].

A commercially available salt-hydrate phase change material (PCM) to create a commercial storage method for cold thermal energy is studied [18]. This article examines the process of charging, the amount of cold given for each setup, as well as the time required for the systems to keep indoor temperatures within an acceptable range. Particularly, salt-hydrates are viewed as a promising material and are consequently widely used in industry. Salt hydrates experience issues with phase segregation and subcooling at low temperatures because they begin to crystallize at a temperature significantly below the melting point, rather than immediately solidify when cooled below the melting point. This is known as subcooling. Without nucleation, the material will only retain perceptible heat and the latent heat will not be released [18].

In a comprehensive review, Du et al. [19] investigated the applications of PCMs for energy generation, heating, and cooling. They came to the following conclusions: The majority of PCMs are organic chemicals suitable for low temperature ranges (20 to 5°C). Salt hydrates and organic compounds are often the PCMs

chosen for the medium low temperature range (5 to 40°C). The main organic PCMs used for medium temperature range (40 to 80°C) are paraffin and fatty acids, and their use as a TES cooling system for electric devices increased their lifespan and operating efficiency by up to 26% and 300%, respectively. And lastly, molten salt has long dominated the TES sector in the high temperature range (80 to 200°C) because of its durability and economic benefits [19].

## 2. Methodology

In this project, the TES tank model comprises the tube for heat transfer fluid delivery was prepared with various tube diameters and lengths. Basically, based on Figure 1, two types of pipes were utilized, the U-tube pipe and a pipe with three elbows combined into a single configuration. These pipe arrangements were chosen based on their compatibility with the project's specifications. CAD software was utilized to create these complex structures. After that, the models were assembled to create a single model. All models' generation and assembly are done in CATIA.

These five models including the tank, U-tube pipe, and three elbow pipes were designed and remained consistent, while the diameter and length of the pipe's dimensions were varied as details shown in Table 1. These individual models were then combined into one integrated model, representing the complete system. This approach allowed for a comprehensive analysis and evaluation of the thermal energy storage system's performance.

To initiate the meshing process, the assembled model comprising the TES tank, U-tube pipe, and the pipe with three elbows were combined and imported into the ANSYS software. Prior preparations were made on this model to ensure suitability for meshing. The size of the meshing elements in the model was adjusted by changing the resolution setting to 2, selected from the preset settings available, resulting in a finer mesh. Additionally, the span angle 'centre' was set for a coarser resolution. Using these settings, the nodes and elements were generated accordingly as example shown in Figure 2, forming the mesh structure. This approach allows for control over the density and distribution of nodes and elements, influencing the accuracy and efficiency of the mesh in capturing the desired physics during the simulation.

The initialization process in ANSYS CFX involves setting the initial values for different parameters to establish a starting point for the simulation. In this case, the values of U (velocity in the x-direction), V (velocity in the y-direction), and W (velocity in the z-direction) are set to 0 m/s, indicating no initial flow or motion. The static pressure was set as 0 Pa since there is no initial pressure difference in the system. The global initial temperature was set as -2°C, representing the condition of the overall starting temperature. Additionally, the mass fraction was set to 1, indicating a fully saturated condition (as for fully solidified PCM0 or ice) for the specific component being simulated. These initial values provide a consistent starting point for the simulation and a constant baseline for the analysis.

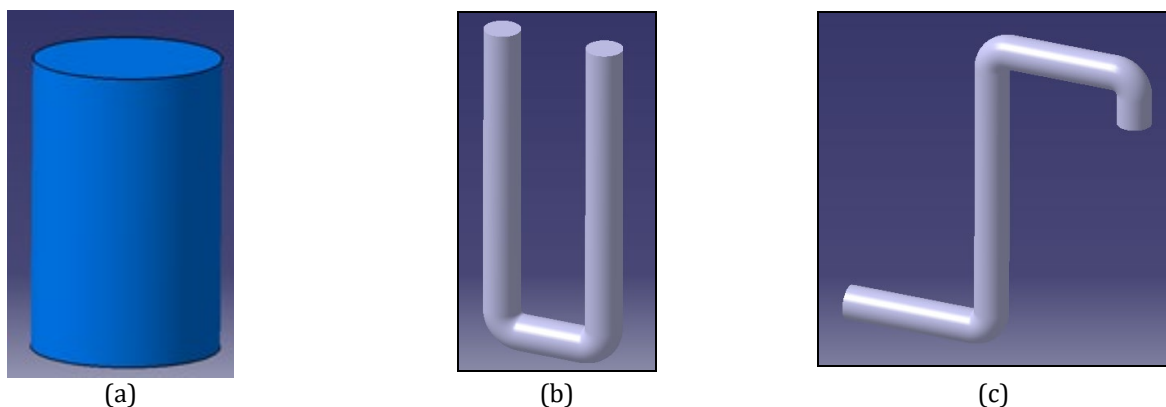


**Fig. 1** Separated 3D model of tube typed TES (a) TES tank; (b) U-tube pipe; (c) Three elbow pipes

**Table 1** The dimension of the models

Model	U-tube pipe	TES tank	3 elbow pipes
First	6.8cm x 60cm		
Second	5.8cm x 65cm		Length 1 – 10cm
Third	5.0cm x 70cm	58cm x 90cm	Length 2 – 30cm
Fourth	4.4cm x 75cm		Length 3 – 60cm
Fifth	3.8cm x 80cm		Length 4 – 30cm

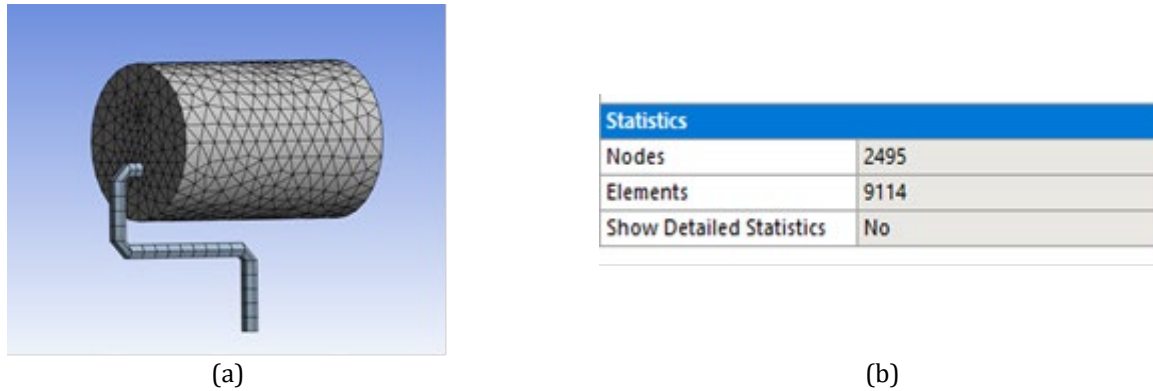


**Fig. 2** Statistic structure for Model 2 (a) TES tank mesh structure; (b) Mesh statistics of the model

### 3. Results and Discussions

One hundred maximum iterations for each simulation was set, providing a limit for the solver to converge and find a solution. The residual target or the convergence criteria was defined as  $1 \times 10^{-4}$  for the project based on Aziz et al. [6] indicating the desired level of accuracy [20]. The solver continues iterating until the residuals reach or fall below this target, ensuring the solution meets the desired accuracy. These settings play a crucial role in controlling the convergence of the solver and ensuring reliable results for the simulation. After completing the simulation, the obtained results were assessed to determine whether the solution had converged. Convergence in this context refers to the state where the solution has reached a desired level of accuracy and stability. Figure 3 shows the example of convergence results for each ANSYS simulation. Model 2 is almost not to reach convergence when compared to the other models that can easily satisfy the convergence criteria.

The investigation of the TES tank involved five different models, each exhibiting a constant temperature at a specific point during the discharging process. The graph shown in Figure 4 reveals that all five models experienced a very minor increase in temperature before reaching a certain point where the temperature stabilized and remained constant. This is explained as at the start of each simulation all errors are higher at the earlier time steps as shown in Figure 3. Based on Figure 4, the behaviour of each model during the melting phase can be analysed. The data shows that all the models ultimately reach a constant temperature of  $0^{\circ}\text{C}$ , indicating the melting phase. Yet, each model exhibits different time intervals required to reach this steady state. Model 1 reaches the steady temperature the fastest, taking 2044 seconds, followed closely by Model 2 at 2178 seconds, while Model 3 takes a bit longer at 2355 seconds. Meanwhile, Model 4 needs even more time, reaching the steady temperature at 2622 seconds, then Model 5 takes the longest at 2755 seconds.

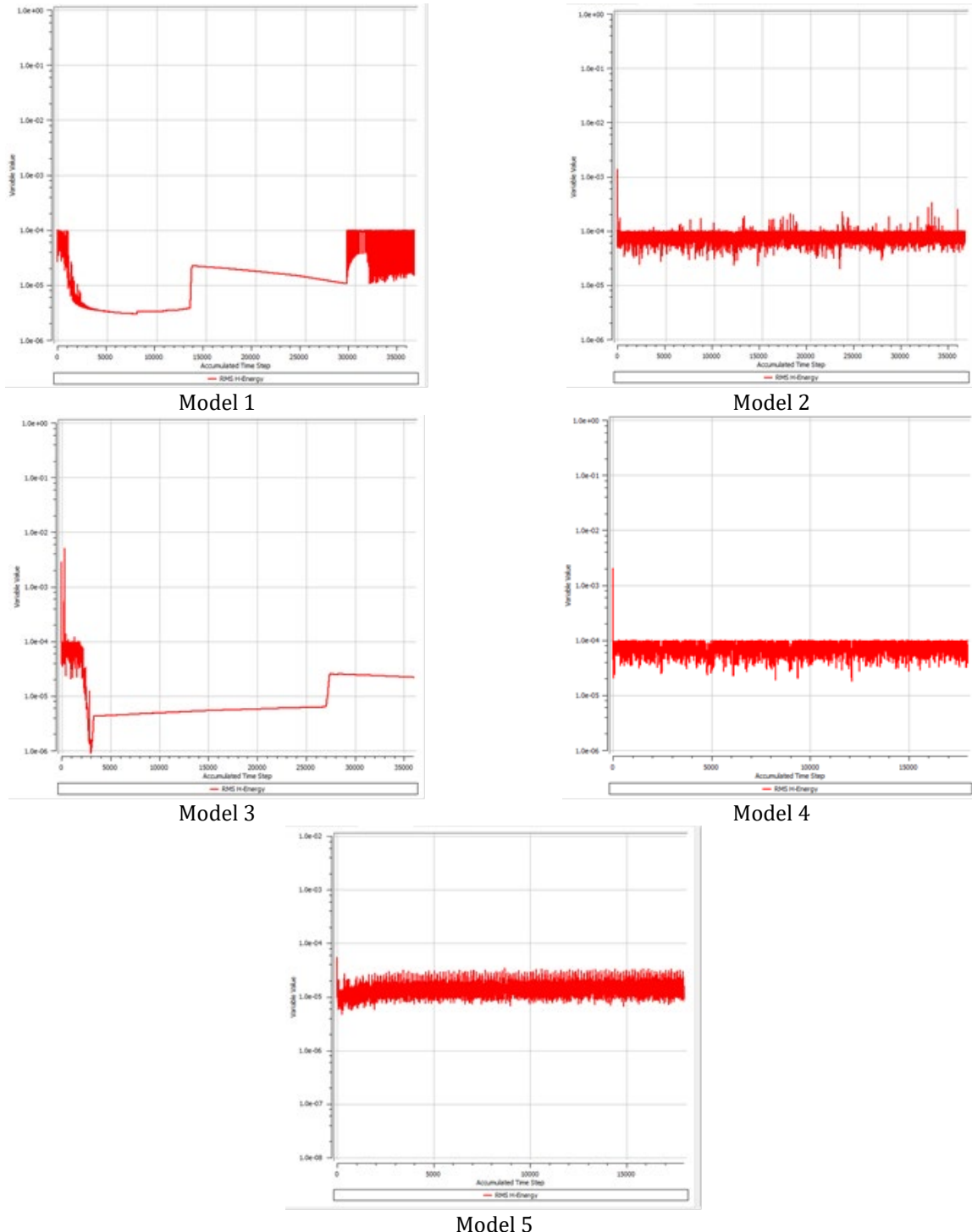
Figure 5 shows the ice mass fraction and the temperature in the TES tank for the Models 1 to 5. For Model 1, the overall ice mass fraction in the tank is 0.9968, which is close to 1, meaning that 99.68% of the material is still in solid ice condition. The remaining 0.32% had a phase change and turned into liquid water. Based on these results, it can be said that, for Model 1, only a little amount of ice has melted during the allotted simulation time, and there is still a significant portion of ice remaining to be melted. For the temperature, the model shows a colour change that it reaches 276.0 K ( $2.85^{\circ}\text{C}$ ) all around the pipe in the TES tank. This indicates that the temperature in the tank has increased, which leads to the melting of the ice. The ice mass fraction for Model 2 is 0.997, as shown in Figure 5 (b), meaning that 99.7% of the substance in the tank is still in the form of solid ice. The remaining 0.3% is the fraction of the mixture that has changed phases and turned into liquid water. This implies that this model's melting percentage is lower than Model 1's. Additionally, the tank's temperature, which remains at 271.1 K ( $-2.05^{\circ}\text{C}$ ), shows that there has not been a major rise in temperature that would have allowed for considerable ice melting.

According to Model 3 as shown in Figure 5 (c), the ice mass fraction of 0.9984, around 99.84% of the substance in the tank is still in the solid ice state. About 0.16% of the total has undergone a phase change and became liquid water. This shows that this model's melting is slightly less extensive than that of earlier models. The tank's constant temperature reading of 271.1K ( $-2.05^{\circ}\text{C}$ ) shows that there is not a considerable change in temperature that would allow for major ice melting.

In Model 4 (Figure 5 (d)), the ice mass fraction is 0.9983, indicating that most of the material (about 99.83%) in the tank remains in the solid ice state. An approximate 0.17% of the material has melted around the pipe, undergoing a phase change to liquid water. This level of melting is similar to what has been observed in the previous model. The temperature around the pipe in the tank was recorded as 272.7K ( $-0.45^{\circ}\text{C}$ ), which shows a slight improvement compared to the previous models. This temperature rise may contribute to the ongoing melting process, gradually transforming more ice into liquid water.

Figure 5 (e) shows that the temperature distributions for Model 5. The ice mass fraction is measured at 0.9992, indicating that most of the tank's contents, approximately 99.92%, remain as ice, with only a small portion, about 0.08%, has transitioned into liquid water through the phase change process. The temperature was recorded around the pipe inside the tank at 272.6K (-0.55 °C), maintaining the same range as the previous model. These temperature conditions help sustaining the frozen part of PCM, thus extensive melting is avoided while system stability is secured.

These results suggest the differences in the melting performance and energy transfer effectiveness between all the models. A more inclusive analysis is needed to find the specific factors contributing to these variations, including the model geometry, material properties, and mechanism of heat transfer. The temperature versus time step data provides a useful insight into the dynamic behaviour of the models during the phase of melting, enabling further investigation and optimization of the system for an efficient energy storage.



Model 5  
**Fig. 3** Convergence results for all models

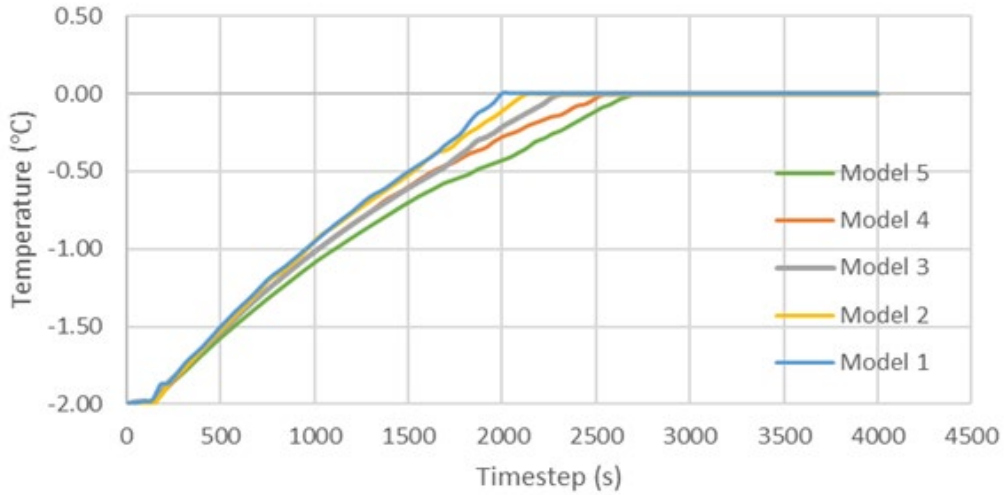
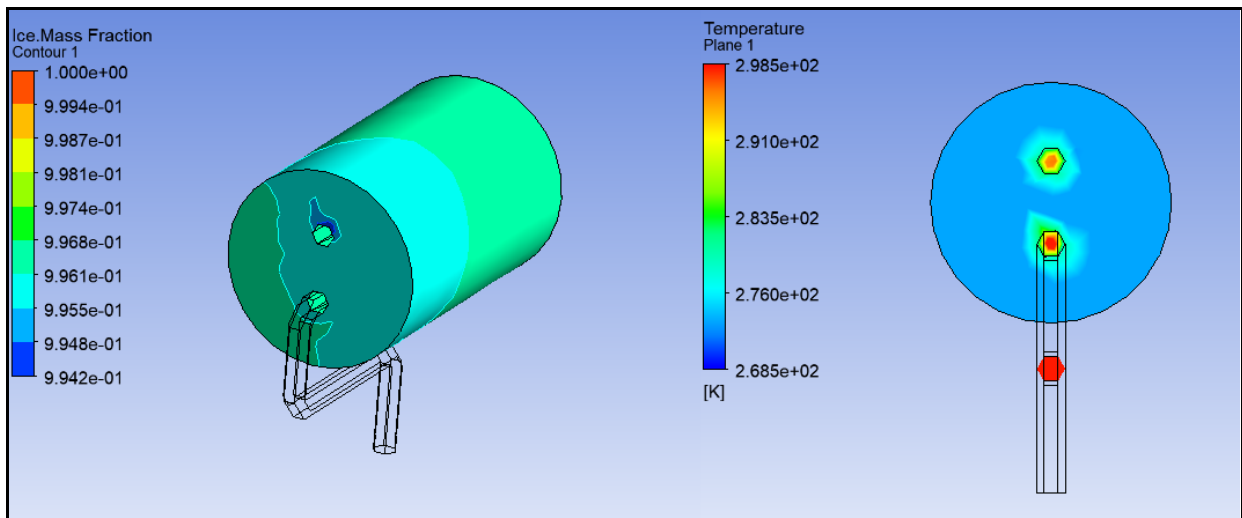
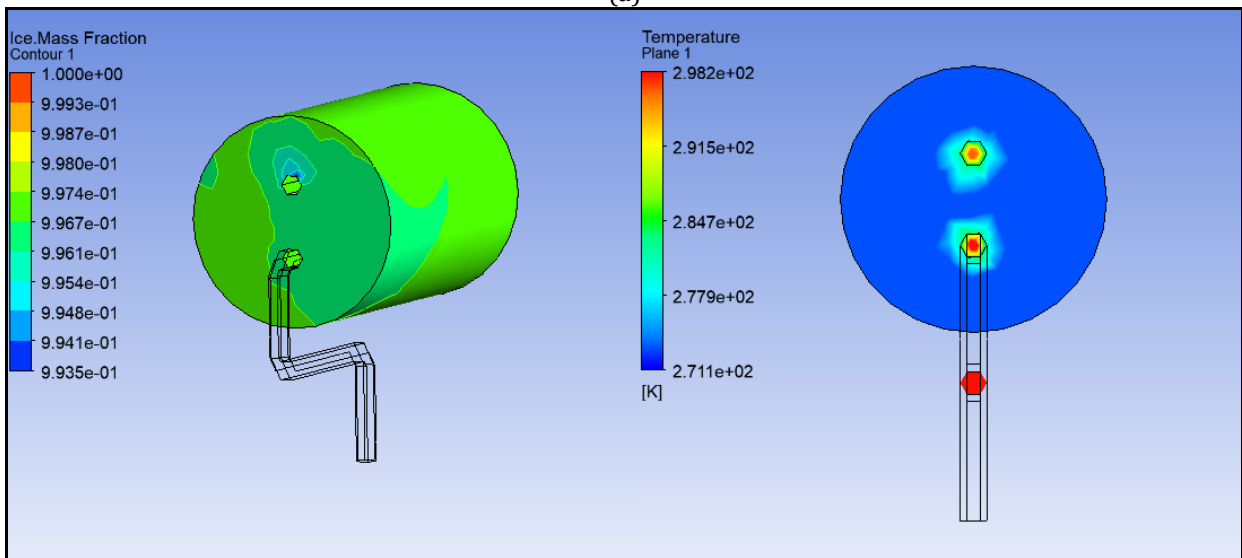


Fig. 4 The temporal evolution of PCM temperature in TES tank

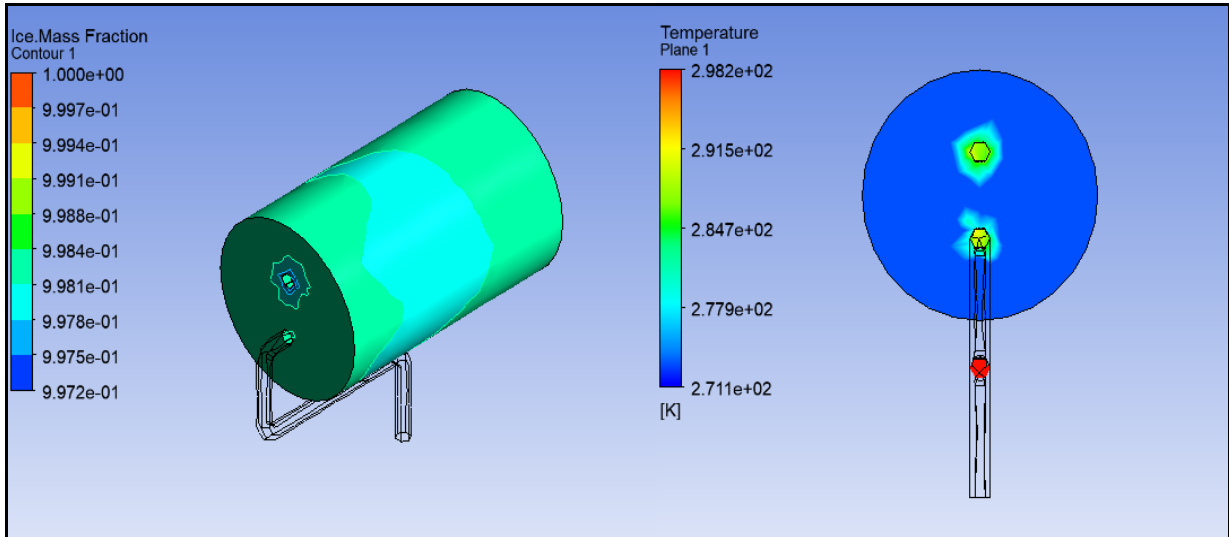


(a)

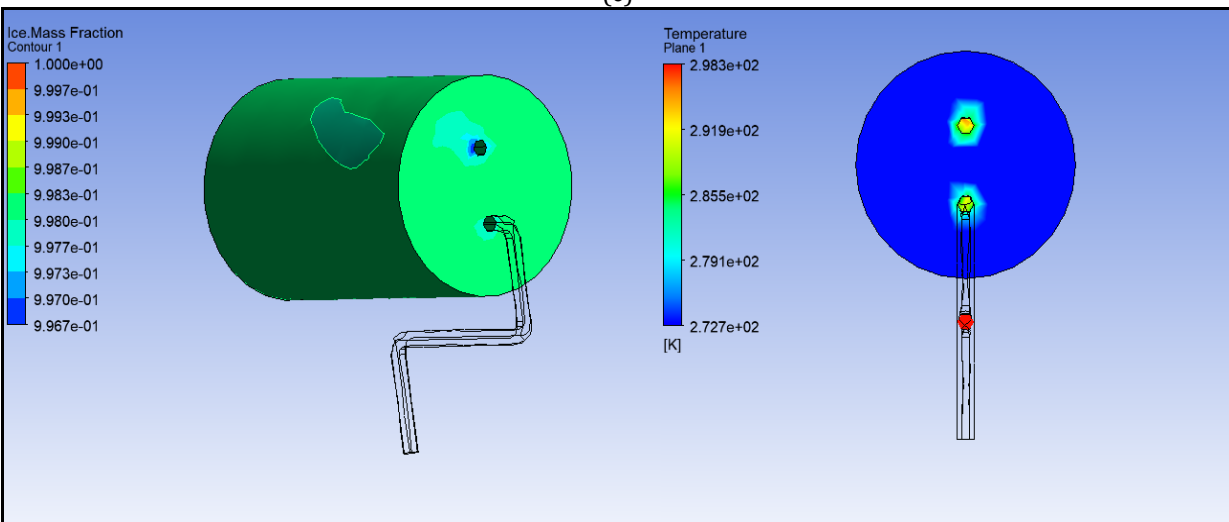


(b)

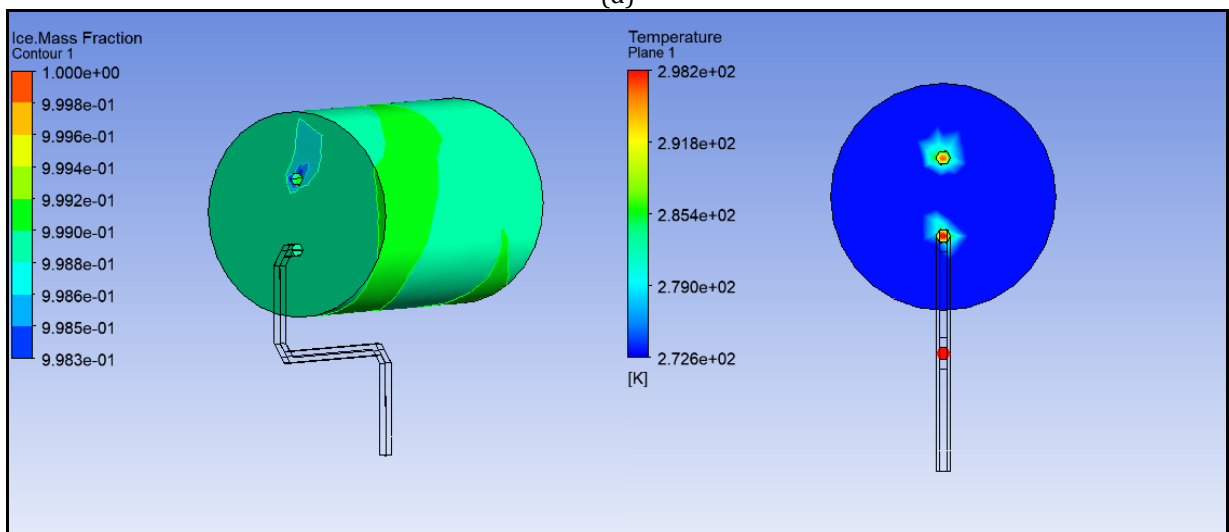
Fig. 5 Ice mass fractions and the temperature distributions for (a) Model 1; (b) Model 2; (c) Model 3; (d) Model 4; (e) Model 5



(c)



(d)



(e)

Fig. 5 Ice mass fractions and the temperature distributions for (a) Model 1; (b) Model 2; (c) Model 3; (d) Model 4; (e) Model 5 (contd.)

#### 4. Conclusion

Convergence test was conducted for all five models to confirm the results attained via ANSYS simulation. The temperature and ice mass fraction are the two important criteria involved in the TES tank performance

assessment. The investigation of the TES tank utilizing five different models has shown that each model reaches a constant temperature of 0°C during the melting phase, however during different time intervals. Model 1 reaches this temperature first, followed by Model 2, Model 3, Model 4, and finally Model 5.

These variations denote differences in melting performance and energy transfer efficiency among the models. A model that reached the constant temperature first signalled a more efficient discharging process, as it indicates a much faster rate of ice melting and thermal energy release. In regard of the ice mass fraction, which represented by the percentage of the remaining solid ice in the tank, Model 1 had the lowest ice mass fraction of 0.9968, signifying that a significant amount of ice persisted but with some noticeable melting. Conversely, Model 5 had the highest ice mass fraction of 0.9992, indicating minimal melting and a greater retention of solid ice. Considering both criteria Model 1 outperformed the others by reaching the constant temperature faster and securing a quite significant amount of solid ice in the TES tank. This means that Model 1 melted the ice faster while still retaining a substantial portion of it. Therefore, Model 1 can be considered the most efficient in terms of energy storage, as it efficiently used the thermal energy and preserved quite a substantial amount of ice in the tank. The faster temperature rise suggested a more effective utilization of thermal energy and a quicker melting rate of the ice. Thus, Model 1 stood out as the superior configuration amongst the model when taking the constant temperature and the ice mass fraction and ease of convergence factors into consideration.

To conclude, the procedures run in this study is managed to assess the performance of TES tanks with different size of the pipe with the fixed volume of cylindrical tank. Simulations were conducted to identify the model that demonstrated the best performance among the five models based on the ease of convergence in simulation.

## Acknowledgement

The authors would like to acknowledge the support from the Fundamental Research Grant Scheme (FRGS) under a grant number FRGS/1/2023/TK08/UNIMAP/02/11 from the Ministry of Higher Education Malaysia (MOHE).

## Conflict of Interest

The authors declare that there is no conflict of interests regarding the publication of the paper.

## Author Contribution

*The authors confirm contribution to the paper as follows: **study conception and design:** N.A.M. Amin, M.S.A. Fouzi, M.S. Bakar, M.A. Karim; **data collection:** M.S. Bakar, M.A. Karim; **analysis and interpretation of results:** A. Mohamad, M.S. Mohamad, M.H. Basha; **draft manuscript preparation:** M.S.A. Fouzi, N.A.M. Amin, A.A. Rahman, I. Zaman. All authors reviewed the results and approved the final version of the manuscript.*

## References

- [1] Zhou, F., Ji, J., Yuan, W., Zhao, X., & Huang, S. (2019). Study on the PCM flat-plate solar collector system with antifreeze characteristics. *International Journal of Heat and Mass Transfer*, 129, 357–366. <https://doi.org/10.1016/j.ijheatmasstransfer.2018.09.114>
- [2] Liu, J., Zhou, Y., Yang, H., & Wu, H. (2022). Net-zero energy management and optimization of commercial building sectors with hybrid renewable energy systems integrated with energy storage of pumped hydro and hydrogen taxis. *Applied Energy*, 321, 119312. <https://doi.org/10.1016/j.apenergy.2022.119312>
- [3] Pan, C., Vermaak, N., Wang, X., Romero, C., & Neti, S. (2021). A fast reduced model for a shell-and-tube based latent heat thermal energy storage heat exchanger and its application for cost optimal design by nonlinear programming. *International Journal of Heat and Mass Transfer*, 176, 121479. <https://doi.org/10.1016/j.ijheatmasstransfer.2021.121479>
- [4] Liang, H., Niu, J., & Gan, Y. (2020). Performance optimization for shell-and-tube PCM thermal energy storage. *Journal of Energy Storage*, 30, 101421–101421. <https://doi.org/10.1016/j.est.2020.101421>
- [5] Wołoszyn, J., Szopa, K., & Czerwiński, G. (2021). Enhanced heat transfer in a PCM shell-and-tube thermal energy storage system. *Applied Thermal Engineering*, 196, 117332. <https://doi.org/10.1016/j.applthermaleng.2021.117332>
- [6] Aziz, S., Amin, N. A. M., Majid, M. A., Belusko, M., & Bruno, F. (2018). CFD simulation of a TES tank comprising a PCM encapsulated in sphere with heat transfer enhancement. *Applied Thermal Engineering*, 143, 1085-1092. <https://doi.org/10.1016/j.applthermaleng.2018.08.013>
- [7] Chen, C. Q., Diao, Y., Zhao, Y., Wang, Z. Y., Liang, L., Wang, T. Y., Zhu, T., & Ma, C. (2020). Thermal performance of a closed collector-storage solar air heating system with latent thermal storage: An experimental study. *Energy*, 202, 117764–117764. <https://doi.org/10.1016/j.energy.2020.117764>

- [8] Jouhara, H., Żabnieńska-Góra, A., Khordehghah, N., Ahmad, D., & Lipinski, T. (2020). Latent thermal energy storage technologies and applications: A review. *International Journal of Thermofluids*, 5, 100039. <https://doi.org/10.1016/j.ijft.2020.100039>
- [9] Wang, Q., Zhou, D., Chen, Y., Eames, P., & Wu, Z. (2020). Characterization and effects of thermal cycling on the properties of paraffin/expanded graphite composites. *Renewable Energy*, 147, 1131-1138. <https://doi.org/10.1016/j.renene.2019.09.091>
- [10] Alam, P., Gupta, N. K., & Nizam, A. R. (2020). Characterization of nanoparticles embedded phase change materials. *Materials Today: Proceedings*, 26, 2932-2937. <https://doi.org/10.1016/j.matpr.2020.02.606>
- [11] Banoqitah, E., Sathyamurthy, R., Moustafa, E. B., Fujii, M., Sudalaimuthu, P., Djouider, F., & Elsheikh, A. H. (2023). Enhancement and prediction of a stepped solar still productivity integrated with paraffin wax enriched with nano-additives. *Case Studies in Thermal Engineering*, 49, 103215-103215. <https://doi.org/10.1016/j.csite.2023.103215>
- [12] Kuziel, A. W., Dzido, G., Turczyn, R., Jędrysiak, R. G., Kolanowska, A., Tracz, A., Zięba, W., Cyganiuk, A., Terzyk, A. P., & Boncel, S. (2021). Ultra-long carbon nanotube-paraffin composites of record thermal conductivity and high phase change enthalpy among paraffin-based heat storage materials. *Journal of Energy Storage*, 36, 102396-102396. <https://doi.org/10.1016/j.est.2021.102396>
- [13] Ghafari, S., Khorshidi, J., Niazi, S., & Samari, F. (2021). Melting study of nano-enhanced phase change material (NePCM) inside a sphere by using of image processing and volume shrinkage methods. *Journal of Energy Storage*, 44, 103376-103376. <https://doi.org/10.1016/j.est.2021.103376>
- [14] Kabeel, A. E., Sathyamurthy, R., Manokar, A. M., Sharshir, S. W., Essa, F. A., & Elshiekh, A. H. (2020). Experimental study on tubular solar still using Graphene Oxide Nano particles in Phase Change Material (NPCM's) for fresh water production. *Journal of Energy Storage*, 28, 101204-101204. <https://doi.org/10.1016/j.est.2020.101204>
- [15] Zhang, Y., Feng, D., Liu, Q., Wang, X., Li, K., Su, J., Zhang, X., & Feng, Y. (2022). Paraffin wax with an addition of nano TiO<sub>2</sub>: Improve thermal and photothermal performances with little decreased latent heat. *Solar Energy*, 246, 273-280. <https://doi.org/10.1016/j.solener.2022.09.052>
- [16] Prabhu, B., & ValanArasu, A. (2020). Stability analysis of TiO<sub>2</sub>-Ag nanocomposite particles dispersed paraffin wax as energy storage material for solar thermal systems. *Renewable Energy*, 152, 358-367. <https://doi.org/10.1016/j.renene.2020.01.043>
- [17] Nazir, H., Batool, M., Ali, M., & Kannan, A. M. (2018). Fatty acids based eutectic phase change system for thermal energy storage applications. *Applied Thermal Engineering*, 142, 466-475. <https://doi.org/10.1016/j.applthermaleng.2018.07.025>
- [18] Tan, P., Lindberg, P., Eichler, K., Löveryd, P., Johansson, P., & Kalagasidis, A. S. (2020). Effect of phase separation and supercooling on the storage capacity in a commercial latent heat thermal energy storage: Experimental cycling of a salt hydrate PCM. *Journal of Energy Storage*, 29, 101266. <https://doi.org/10.1016/j.est.2020.101266>
- [19] Du, K., Calautit, J., Wang, Z., Wu, Y., & Liu, H. (2018). A review of the applications of phase change materials in cooling, heating and power generation in different temperature ranges. *Applied energy*, 220, 242-273. <https://doi.org/10.1016/j.apenergy.2018.03.005>
- [20] Shahril, S. M., Quadir, G. A., Amin, N. A. M., & Badruddin, I. A. (2017). Thermo hydraulic performance analysis of a shell-and-double concentric tube heat exchanger using CFD. *International Journal of Heat and Mass Transfer*, 105, 781-798. <http://dx.doi.org/10.1016/j.ijheatmasstransfer.2016.10.021>